International Journal of Current Engineering and Technology
E-ISSN 2277 – 4106, P-ISSN 2347 – 5161

Available at http://inpressco.com/category/ijcet

Research Article

Calculation of Distribution of Stress Micro Electro-Mechanical System by using Finite Element Method

Mohammad Qasim Abdullah[#], Hatem R. Wasmi[#], Jasim Mohammad Abid[#] and Omar Ali Jassim[#*]

[#]University of Baghdad, Mechanical Dept., Iraq

Accepted 02 Nov 2016, Available online 05 Nov 2016, **Vol.6, No.6 (Dec 2016)**

Abstract

It was used ANSYS Program in the case study, that describes the problem, a static analysis is carried out. Figure (4) shows the Von Misses stress distribution obtained with 24 bilinear quadrilateral elements. It should be noted here that 24 elements (41 nodes) for such a problem may not be sufficient for accurate results. Analyses with a denser mesh (129 elements and 185 nodes) using the same element type are also carried out. Their input files will be similar to that shown, but with more nodes and elements Figures (5) and (6) show the Von Misses stress distribution obtained using 96 (129 nodes) and 144 elements (185 nodes), respectively. Figure (7) also shows the results obtained when 24 eight-nodal elements (105 nodes in total) are used instead of four-nodal elements. The element types in ANSYS are for eight nodal, plane stresses. Finally, linear, triangular elements are also used for comparison, and the stress distribution obtained is shown in Figure (8).

Keywords: *Distribution of Stress, FEM etc.*

Introduction

A common micro-actuator in the form of a side drive electrostatic micro-motor, as shown in Figure (1) [GR Liu and SS Quek, 2013]. Such micro-motors are usually made from poly-silicon using lithographic techniques. Their diameters vary depending on the design, with the first designs having diameters of 60–120 μm. Of course the actual working dynamics of the micro-motor will be rather complex to model, though it can still be readily done if required.

Figure 1 SEM image of an electrostatic micro-motor with eight rotor and 12 stator poles

*Corresponding author **Omar Ali Jassim** and **Jasim Mohammad Abid** are Ph.D. student; **Mohammad Qasim Abdullah#, Hatem R. Wasmi** are working as Professors

Therefore, to illustrate certain points pertaining to the use of basic 2D solid elements, we basically use the geometrical and material information for this micro-motor and apply arbitrary loading and boundary conditions to it. Isotropic material properties will be employed here to makes things less complicated.

The material properties of poly-silicon are shown in Table(1) [Timoshenko, S. P. and Goodier, J. N.,1970]. We shall do a stress analysis on the rotor with some loading condition on the rotor blades. Examining the rotor in Figure 1, we can see that it is symmetrical, i.e. we need not model the full rotor, but rather we can just model say one quarter of the rotor and apply the necessary boundary conditions. We can do this since this one-quarter model will be repeated /model and the results will be the same if the condition of repetition is properly applied. Hence, this becomes a neat and efficient way of modeling repetitive or symmetrical geometry.[Cook, R. D.,1995]

Table.1. Elastic properties of poly-silicon [Timoshenko, S. P. and Goodier, J. N.,1970]

Young's Modulus, E	169 GPa
Poisson's ratio, ν	0.262
Density, ρ	2300 kgm−3

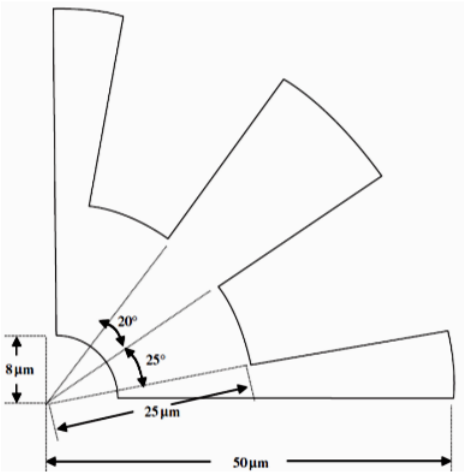

Figure 2 Plan view (2D) of a quarter of micro-motor rotor

System Modeling

Figure 2 shows the one-quarter model of the micro-motor rotor. We take the diameter of the whole rotor to be 100 µm and the depth or thickness to be 13µm, to correspond with realistic values of micro-motor designs. The geometry can be easily drawn using preprocessors like patran or using basic CAD software, after which it can be imported into preprocessors for meshing. Note that preprocessors are software used to aid us in visualizing the geometry, and to mesh up the geometry using finite elements[Liu, G. R., 2002], especially for complicated geometries. To illustrate the formulation of the finite element equations clearly, we would initially mesh up the geometry in Figure (2) with a very sparse mesh, as shown in Figure (3) [Liu, G. R., 2002].

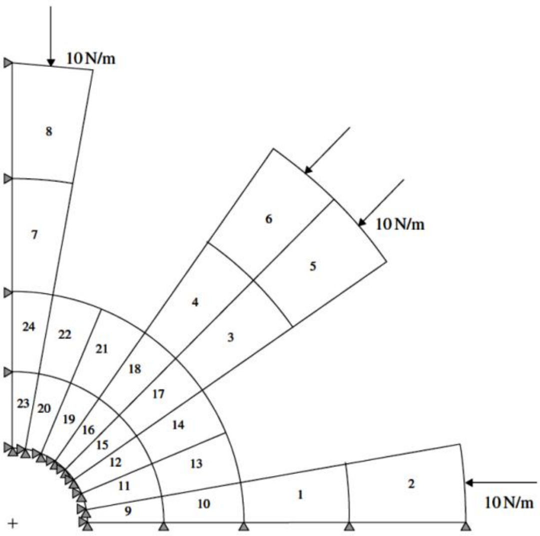

Figure 3 Finite element mesh with (24) 2D quadrilateral , for nodal element

Four nodal, quadrilateral elements are used with a total of 24 elements and 41 nodes in the model.

We shall increase the number of elements (and nodes) in later analyses to compare the results. Since the depth or thickness of the motor is much smaller than the other dimensions, and the external forces are assumed to be within the plane of the rotor, we can assume plane stress conditions.

In the above figure, it can also be seen that a distributed force of 10 N/m is applied compressively to the rotor blades. The centre hole in the rotor which is supposed to be the location for a 'hub' to keep the rotor in place is assumed to be constrained. The nodes along the edge $y = 0$ are constrained in the y direction and the nodes along the edge $x = 0$ are constrained in the x direction. These are to simulate the symmetrical boundary conditions of the model, since those nodes are not supposed to move in the direction normal to the plane of symmetry. Similarly, if we are to model a one-eighth model, such rules for symmetry apply except that one of the planes of symmetry will be the line $y = x$.

Solution Process

Let us now try to relate the information we provided in the input file. the first sets of data usually defined are the nodes and their coordinates. Then, there are the element cards containing the connectivity information. The importance of this information has already been mentioned in previous case studies. Looking at Figure 3[Liu, G. R., 2002], it is not difficult to guess that the element used is an isoperimetric quadrilateral element, rather than that of a rectangular element. Obviously, it can be visualized that using rectangular elements would pose a problem in meshing the geometry here. In fact, the use of purely rectangular elements is so rare that most software only provides the more versatile quadrilateral element [Zienkiewicz, O. C., and Taylor , 2000]. This information from the nodal and element cards will be used for constructing the element matrices (Eqs. (1) and (2)) [Rao, S.S.,1999 and Reddy, J. N.,1993] .

$$\mathbf{k}_e = \int_{-1}^{+1}\int_{-1}^{+1} h\mathbf{B}^{\mathrm{T}}\mathbf{c}\mathbf{B}\,\det|\mathbf{J}|\,\mathrm{d}\xi\,\mathrm{d}\eta \qquad (1)$$

$$\begin{aligned}\mathbf{m}_e &= \int_V \rho\mathbf{N}^T\mathbf{N}\mathrm{d}V = \int_A\int_0^h \mathrm{d}x\rho\mathbf{N}^T\mathbf{N}\,\mathrm{d}A = \int_A h\rho\mathbf{N}^T\mathbf{N}\,\mathrm{d}A \\ &= \int_{-1}^{+1}\int_{-1}^{+1} h\rho\mathbf{N}^T\mathbf{N}\,\det|\mathbf{J}|\,\mathrm{d}\xi\,\mathrm{d}\eta\end{aligned} \qquad (2)$$

Next, the property cards define the properties of the elements, and also specify the material, the elements should possess. For the plane stress elements, the thickness of the elements must be specified (13µm in this case)[Cook, R. D.,1995], since it is required in the stiffness and mass matrices (the mass matrix is actually not required in the concern case study, since this is a static analysis). Similarly, the elastic properties of the poly-silicon material defined in the material card are also required in the element matrices. It should be noted that in ANSYS, the integral in Eq. (1) is evaluated using the Gauss integration scheme, and the default number of Gauss points for the bilinear element is 4.

The boundary cards (BC cards) define the boundary conditions for the model. To model the symmetrical boundary conditions, at the lines of symmetry (x = 0 and y = 0), the nodal displacement component normal to the line is constrained to zero. The nodes (node set, FIXED) along the centre hole where the hub should be is also fully clamped in. The load cards defined specify the distributed loading on the motor, as shown in Figure 3. These will be used to form the force vector, which is similar in form to that of Eq. (3) [Rao, S.S.,1999 and Reddy, J. N.,1993].

$$\mathbf{f}_e = \int_l [\mathbf{N}]^{\mathrm{T}}\Big|_{2\text{-}3} \begin{Bmatrix} f_{sx} \\ f_{sy} \end{Bmatrix} \mathrm{d}l \qquad (3)$$

The control cards are used to control the analysis, which in this case defines that this is a static analysis. Finally, the output cards define the necessary output requested, which here are the displacement components, the stress components and the strain components. Once the input file has been created, one can then invoke ANSYS to execute the analysis [Y. Nakasone and S. Yoshimoto,2006], and the results will be written into an output file that can be read by the postprocessor.

Results and Discussion

Using the above ANSYS input file that describes the problem [Y. Nakasone and S. Yoshimoto,2006], a static analysis is carried out. Figure (4) shows the Von Misses stress distribution obtained with 24 bilinear quadrilateral elements. It should be noted here that 24 elements (41 nodes) for such a problem may not be sufficient for accurate results. Analyses with a denser mesh (129 nodes and 185 nodes) using the same element type are also carried out. Their input files will be similar to that shown, but with more nodes and elements

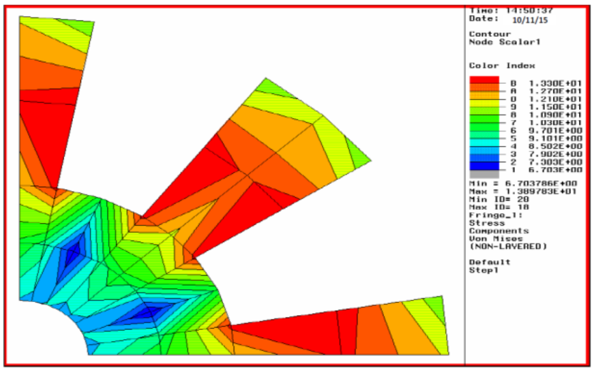

Figure 4 Analysis no. 1: Von Mises stress distribution using 24 bilinear quadrilateral elements

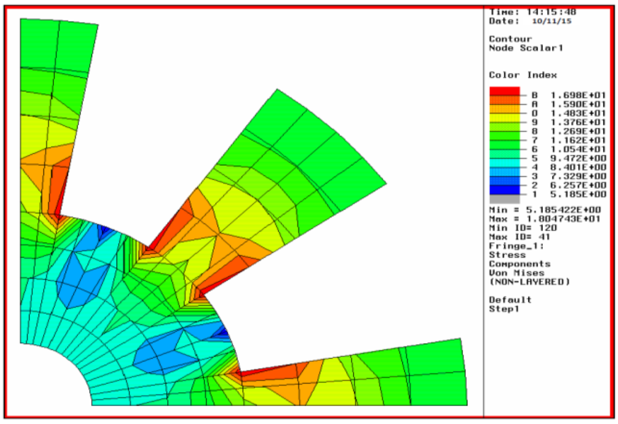

Figure 5 Analysis no. 2: Von Mises stress distribution using 96 bilinear quadrilateral elements

Figures (5) and (6) show the Von Misses stress distribution obtained using 96 (129 nodes) and 144 elements (185 nodes), respectively. Figure (7) also shows the results obtained when 24 eight-nodal elements (105 nodes in total) are used instead of four-nodal elements. The element type in ANSYS for eight nodal, plane stress, quadratic element is 'CPS8'. Finally, linear, triangular elements are also used for comparison, and the stress distribution obtained is shown in Figure (8).From the results obtained, it can be noted that analysis 1, which uses 24 bilinear elements, does not seem as accurate as the other three. Table.3 shows the maximum Von Misses stress for the five analyses. It can be seen that the maximum Von Misses stress using just 24 bilinear, quadrilateral elements (41 nodes) is just about 0.0139 GPa, which is a bit low when compared with the other analyses. The other analyses, especially from analyses 2 to 4 using quadrilateral elements, obtained results that are quite close to one another when we compare the maximum Von Misses stress. We can conclude that using just 24 bilinear, quadrilateral elements is definitely not sufficient in this case. The comparison also shows that using quadratic elements (eight-nodal) with a total of 105 nodes, yielded results that are close to analysis 3 with the bilinear elements and 105 nodes. In this case, the quadratic elements also have curved edges, instead of straight edges and this would define the curved geometry better. Looking at the maximum Von Misses stress obtained using triangular elements in analysis 5, we can see that, despite having the same number of nodes as in analysis 2, the results obtained showed some deviation.

This clearly shows that quadrilateral elements in general provide better accuracy than triangular elements. However, it is still convenient to use triangular elements to mesh complex geometry containing sharp corners.

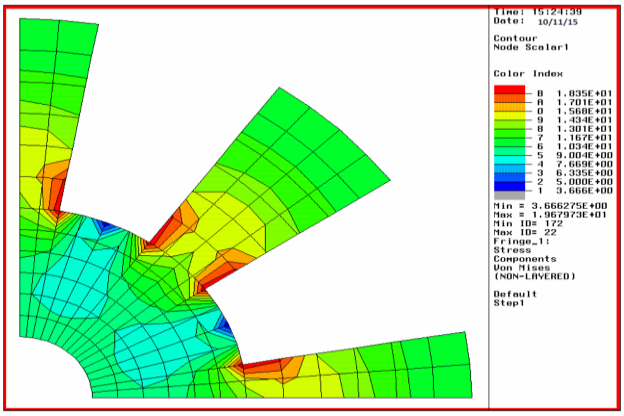

Figure 6 Analysis no. 3: Von Mises stress distribution using 144 bilinear quadrilateral elements

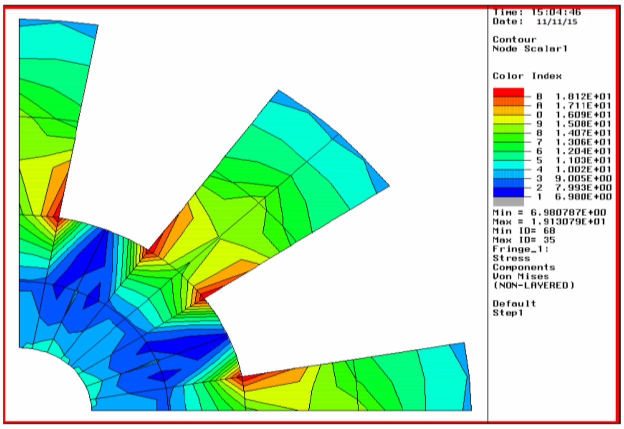

Figure 7 Analysis no. 4: Von Mises stress distribution using 24 eight-nodal, quadratic elements

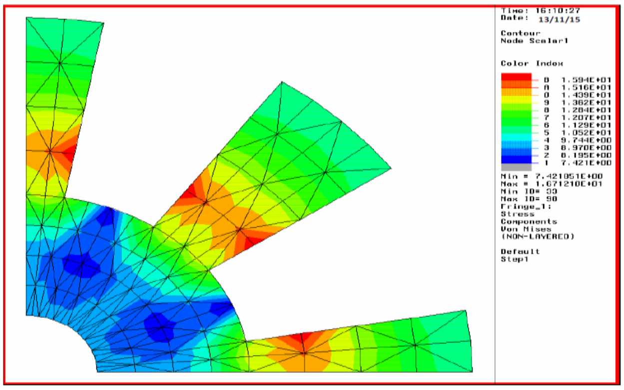

Figure 8 Analysis no. 5: Von Mises stress distribution using 192 three-nodal, triangular elements

Table 3 Maximum Von Misses stress

Analysis no.	Number/type of elements	Total number of nodes in model	Maximum Von Mises stress (GPa)
1	24 bilinear, quadrilateral	41	0.0139
2	96 bilinear, quadrilateral	129	0.0180
3	144 bilinear, quadrilateral	185	0.0197
4	24 quadratic, quadrilateral	105	0.0191
5	192 linear, triangular	129	0.0167

From the stress distribution, it can generally be seen that there is stress concentration at the corners of the rotor structure, as expected. Therefore, if structural failure is to occur, it would be at these areas of stress concentration.

References

G.R Liu and SS Quek , 2013 , The Finite Element Method, A practical course

Timoshenko, S. P. and Goodier, J. N.,1970 , Theory of Elasticity, 3rd edition, McGraw-Hall, New York.

Liu, G. R., 2002, Mesh Free Methods: Moving Beyond the Finite Element Method, CRC Press, Boca Raton.

Cook, R. D.,1995, Finite Element Modeling for Stress Analysis, John Wiley & Sons, Inc.

Rao, S.S.,1999, The Finite Element in Engineering, 3rd edition, Butterworth-Heinemann

Reddy, J. N.,1993, Finite Element Method, John Wiley & Sons Inc., New York

Zienkiewicz, O. C., and Taylor, 2000, The Finite Element Method, 5th edition, Butterworth Heinemann.

Y. Nakasone and S. Yoshimoto,2006, Engineering Analysis With ANSYS Software